Journal of the Arkansas Academy of Science

Volume 61 Article 11

2007

Electron Shock Waves: Ionization Rate and Solutions to the EFD Equations

Mostafa Hemmati
Arkansas Tech University, mhemmati@atu.edu

Steven Summers
Arkansas Tech University

Michael Weller
Arkansas Tech University

Electron Shock Waves: Ionization Rate and Solutions to the EFD Equations

MOSTAFA HEMMATI[1,2], STEVEN SUMMERS[1], AND MICHAEL WELLER[1]

[1]*Department of Physical Sciences, Arkansas Tech University, Russellville, AR 72801*

[2]Correspondence: mhemmati@atu.edu

Abstract.—This paper describes our numerical investigation into ionizing breakdown waves, primarily antiforce waves. Antiforce waves are waves for which the electric field force on the electrons is in the opposite direction of the wave's propagation. This investigation required us to utilize one-dimensional electron fluid-dynamical equations, which were applied to a pulse wave that transmits into a region of neutral gas and is under the influence of an applied electric field. Two important assumptions were made in applying these equations: electrons were considered to be the main component in the propagation of the pulse wave, and the partial pressure of the electron gas provided the driving force for the wave. The pulse waves were considered to be shock-fronted, and these waves are composed of 2 regions: a thin sheath region that exists behind the shock front and a thicker quasi-neutral region that follows the sheath region and in which ionization continues as the electron fluid cools. The set of equations used to investigate these waves consists of the equations of conservation of mass, momentum, and energy coupled with Poisson's equation, which altogether are known as the electron fluid-dynamical (EFD) equations.

Key words:— ionizing breakdown waves, antiforce waves, one-dimensional electron fluid-dynamical equations, Poisson's equation.

Introduction

For ages, lightning was a natural occurrence that baffled humanity. Lightning, however, is merely one example of luminous pulses that are generated by a potential differences occurring between two points in a gas. As one of the first scientists to study the phenomenon, Von Zahn (1879) proposed that there was negligible mass motion within the pulse based on a lack of Doppler shift in the radiation emitted from the breakdown waves. Thomson (1893) later observed that breakdown waves, rather than instantly jumping from one point to another, moved at approximately one-half the speed of light.

Thomson's observations were later proven correct by Beams (1930), who proposed an explanation for the phenomenon: the gas that exists behind the pulse is electrically conductive, which allows for it to carry a potential and create a breakdown of the gas in the area as the wave transmits through. In addition, Beams explained that positive ions in the gas will have an insignificant increase in speed compared to the speed increase for electrons due to the much larger mass of the positive ions. Beams concluded that the potential difference between the two electrodes translates into a very high electric field at the wave front. Behind this wave front and within the sheath region, the space charge field cancels this applied field, causing the net electric field to become zero at the end of the sheath region. This causes the time span of the electric field force to be very brief, though it produces a greater electron acceleration compared to heavy particle acceleration due to the mass difference between the two. The electron gas partial pressure then causes the propagation of the wave front away from the discharge electrode. This explanation is still held to be true to this day.

Paxton and Fowler (1962) then applied a three-fluid (electrons, ions, and neutral particles) hydrodynamical model to devise a set of equations to describe the wave propagation, while at the same time Haberstich (1964) proposed that the luminous pulse be considered fluid-dynamical in nature. Shelton and Fowler (1968) continued this work, describing the phenomena as electron fluid-dynamical waves. Developing a set of one-dimensional equations to describe the phenomena, they derived equations for energy and momentum loss and gain terms during the collision of electrons with heavy particles. Shelton and Fowler focused primarily on proforce waves, which are waves whose electric field force on electrons is in the same direction as the direction of the propagation of the pulse. For the dynamical transition region of the wave, Fowler and Shelton (1974) used an approximation method to solve their set of electron fluid-dynamical equations. Their solutions, though approximations, were in good agreement with the experimental data available (Blais and Fowler 1973).

Sanmann and Fowler (1975) would later try to account for the propagation of antiforce waves. By considering the electron gas partial pressure to be much greater than that of the other species' partial pressures, Sanmann and Fowler proposed that the electron gas partial pressure provided the driving force for the wave's propagation. By adding terms to the equation of conservation of energy, Fowler et al. (1984) completed the set of electron fluid dynamical equations. This would prove essential for exact numerical solution of the entire set of electron fluid-dynamical equations. In addition, they developed a computer program that would allow for integration of the equations through the sheath region. A year later, Hemmati et al. (1985) modified these electron fluid-dynamical equations in order to study other types of breakdown waves. Later, Hemmati (1999) completed the set of electron fluid dynamical equations representing antiforce waves.

Using initial boundary conditions that exist at the wave front, integration of the set of EFD equations through the sheath region for antiforce waves was a success. Integration of the EFD equations, which were modified for the thermal region of the wave, was made possible through that region by using values of

electron gas temperature and number density, ionization rate, and the pre-existing conditions at the end of the sheath region as the initial boundary conditions for the wave's thermal region. The results that followed satisfy the conditions required at the end of the sheath and quasi-neutral regions. A computer program was prepared which calculated the ionization rate at each step of the integration through the sheath region. That computer program was then modified according to the conditions at the end of the sheath region, and the modified program for the ionization rate made the integration of the set of equations possible through the quasi-neutral region. From there, the wave profiles for electric field, electron velocity, electron number density, electron gas temperature, and ionization rate within the sheath and quasi-neutral regions were determined.

Methods

To analyze breakdown waves, the equations that were developed by Fowler et al. (1984) were used: these represent a one-dimensional, steady-state, electron fluid-dynamical wave propagating into a neutral medium at constant velocity. These EFD equations are the equations of conservation of mass, momentum, and energy coupled with Poisson's equation:

$$\frac{d(nv)}{dx} = n\beta, \qquad [1]$$

$$\frac{d}{dx}[mnv(v-V)+nkT_e] = -enE - Kmn(v-V), \qquad [2]$$

$$\frac{d}{dx}[mnv(v-V)^2 + nkT_e(5v-2V) + 2envΦ - \frac{5nk^2T_e}{mK}\frac{dT_e}{dx}]$$
$$= -3(\frac{m}{M})nkKT_e - (\frac{m}{M})Kmn(v-V)^2, \qquad [3]$$

$$\frac{dE}{dx} = \frac{e}{\varepsilon_0}n(\frac{v}{V}-1), \qquad [4]$$

where n, v, Te, e, and m represent the electron number density, velocity, temperature, charge, and mass, respectively, and M, E, E_o, V, k, K, x, β, and ϕ represent the neutral particle mass, electric field within the sheath region, electric field at the wave front, wave velocity, Boltzmann's constant, elastic collision frequency, position within the sheath region, ionization frequency, and ionization potential of the gas.

Reducing the set of electron fluid dynamical equations to a non-dimensional form required the introduction of the following dimensionless variables:

$$\eta = \frac{E}{E_o}, \nu = (\frac{2e\phi}{\varepsilon_o E_o^2})n, \psi = \frac{v}{V}, \theta = \frac{T_e k}{2e\phi}, \xi = \frac{eE_o x}{mV^2},$$
$$\alpha = \frac{2e\phi}{mV^2}, \kappa = \frac{mV}{eE_o}K, \mu = \frac{\beta}{K}, \omega = \frac{2m}{M},$$

in which η, ν, ψ, θ, μ, and ξ represent the dimensionless net electric field of the applied field plus the space charge field, electron number density, electron velocity, electron gas temperature, ionization rate, and position within the sheath region, while α and κ represent wave parameters.

These dimensionless variables are then substituted into equations 1 through 4, yielding

$$\frac{d(\nu\psi)}{d\xi} = \kappa\mu\nu, \qquad [5]$$

$$\frac{d}{d\xi}[\nu\psi(\psi-1)+\alpha\nu\theta] = -\nu\eta - \kappa\nu(\psi-1), \qquad [6]$$

$$\frac{d}{d\xi}[\nu\psi(\psi-1)^2 + \alpha\nu\theta(5\psi-2) + \alpha\nu\psi + \alpha\eta^2 - \frac{5\alpha^2\nu\theta}{\kappa}\frac{d\theta}{d\xi}] =$$
$$-\omega\kappa\nu[3\alpha\theta + (\psi-1)^2], \qquad [7]$$

$$\frac{d\eta}{d\xi} = \frac{\nu}{\alpha}(\psi-1). \qquad [8]$$

Within the wave exists a sheath region and a quasi-neutral region, as proposed by Shelton and Fowler (1968). For the sheath region, the electron velocity starts at an initial value at the shock front and reduces to a speed equivalent to that of a heavy particle. In addition, the electric field goes from a maximum value at the shock front to a negligible value at the trailing edge of the sheath. These conditions translate into the following:

$$\psi_2 = 1, \eta_2 = 0, \psi_2' = 0, \text{ and } \eta_2' = 0, \qquad [9]$$

where ψ_2, η_2, ψ_2', and η_2' represent the non-dimensional electron velocity, electric field, electron velocity derivative, and electric field derivative at the end of the sheath region, respectively.

For the quasi-neutral region, the electron gas cools close to room temperature through the further ionization of neutral

particles, so that the electric field energy present ahead of the wave is converted to ionization energy behind the wave. This leads to the following expected conditions at the end of the quasi-neutral region in non-dimensional form: $\nu_f = 1$ and $\theta_f = 0.065$.

Attempts at integrating equations 5 through 8 through the quasi-neutral region were not successful. These equations were derived by combining the primitive forms of the fluid equations, but because approximation methods were not used to solve the set of fluid equations, the use of the combined form of the equations was not required. As such, to investigate the quasi-neutral region, the primitive form of the electron fluid-dynamical equations was utilized:

$$\frac{d(\nu\psi)}{d\xi} = \kappa\mu\nu, \qquad [10]$$

$$\frac{d}{d\xi}[\nu\psi^2 + \alpha\nu\theta] = -\nu\eta - \kappa\nu(\psi - 1) + \kappa\mu\nu, \qquad [11]$$

$$\frac{d}{d\xi}(\nu\psi^3 + 5\nu\psi\alpha\theta - \frac{5\alpha^2\nu\theta}{\kappa}\frac{d\theta}{d\xi}) =$$
$$-2\nu\psi\eta - 2\kappa\nu(\psi - 1) + \kappa\mu\nu(\psi - 1) - \omega\kappa\nu[3\alpha\theta + (\psi - 1)^2], \qquad [12]$$

$$\frac{d\eta}{d\xi} = \frac{\nu}{\alpha}(\psi - 1). \qquad [13]$$

Applying the expected conditions for the end of the sheath region (equation 9) in the expanded forms of the equations of conservation of mass and momentum (equations 10 and 11) led to the following equations that describe the quasi-neutral region:

$$\nu_2' = \kappa\mu_2\nu_2 \qquad [14]$$

and

$$\theta_2' = -\kappa\mu_2\theta_2 \qquad [15]$$

where $\nu'2$ and $\theta'2$ represent the electron number density derivative and electron gas temperature derivative for the quasi-neutral region.

Integrating equations 5-8 through the sheath region yields the electron number density, electron gas temperature, and ionization rate values at the end of that region, and these values will be used as the initial boundary conditions for the quasi-neutral region. Equations 14 and 15 have been successfully integrated through the quasi-neutral region, yielding results that are in agreement with the expected conditions at the trailing edge of the wave: $\nu_f = 1$ and $\theta_f = 0.065$.

Slight adjustments in the electron-fluid dynamical equations are necessary to apply the equations to antiforce waves. For an observer that is stationary relative to the wave front, the heavy particles in the wave move in the negative x direction ($V < 0$, $E_o > 0$, and $K_1 > 0$). This leads to both κ and ξ being negative. Therefore, antiforce waves have a set of dimensionless variables that differ slightly. As derived by Hemmati (1999), these variables are

$$\eta = \frac{E}{E_o}, \nu = (\frac{2e\phi}{\varepsilon_o E_o^2})n, \psi = \frac{v}{V}, \theta = \frac{T_e k}{2e\phi}, \xi = -\frac{eE_o x}{mV^2},$$
$$\alpha = \frac{2e\phi}{mV^2}, \kappa = -\frac{mV}{eE_o}K, \mu = \frac{\beta}{K}, \omega = \frac{2m}{M}.$$

Hence, the equations that describe the antiforce waves in non-dimensional form are given as follows:

$$\frac{d}{d\xi}[\nu\psi] = \kappa\mu\nu, \qquad [16]$$

$$\frac{d}{d\xi}[\nu\psi(\psi - 1) + \alpha\nu\theta] = \nu\eta - \kappa\nu(\psi - 1), \qquad [17]$$

$$\frac{d}{d\xi}[\nu\psi(\psi - 1)^2 + \alpha\nu\theta(5\psi - 2) + \alpha\nu\psi + \alpha\eta^2 - \frac{5\alpha^2\nu\theta}{\kappa}\frac{d\theta}{d\xi}] =$$
$$-\omega\kappa\nu[3\alpha\theta + (\psi - 1)^2], \qquad [18]$$

$$\frac{d\eta}{d\xi} = -\frac{\nu}{\alpha}(\psi - 1). \qquad [19]$$

Early on in the study of breakdown waves, the ionization rate was assumed to be constant throughout the region in which an electric field is present. Later, Fowler (1983) showed that this assumption of a constant rate was incorrect and subsequently replaced it by a computation that was based on free trajectory theory, yielding the rate of ionization as

$$\beta = N^2 \int \sigma(v_o) f(v_o)\, dv_o\, \sigma_i(v_f) v_f\, e^{-\int_0^{\xi} \alpha N\, d\xi}\, d\xi_o \qquad [20]$$

This computation included ionization from both random and

directed electron motions within the wave. Applying this equation to ionization in a strong field with independent drift velocity, Fowler derived a dimensionless form of the equation. In non-dimensional form, this expression for the ionization rate is given by

$$\mu = \mu_o \int_{1/\sqrt{2\theta}}^{\infty} \sigma_i z^2 dz \int_{B}^{\infty} \frac{e^{-(z-u)^2} - e^{-(z+u)^2}}{u} du\, e^{-2Cu}, \qquad [21]$$

where $B = (1-\psi)/\sqrt{2\alpha\theta}$ and $C = \kappa\sqrt{2\alpha\theta}/\eta$. This function was assumed to be constant by Shelton, and the ionization rate, which changes from accelerational ionization at the front of the wave to directed velocity ionization in the intermediate stages of the wave to thermal ionization at the end of the wave, does remain considerably constant at the beginning of the sheath.

Results

At the wave front, the electron velocity (v_1) is less than the wave velocity (V). Therefore, the dimensionless electron velocity at the wave front, ψ_1, must be less than 1. According to Poisson's equation, this results in the electric field having a positive slope behind the wave front, which leads to an initial increase in the electric field. Traveling through the sheath region following the shock front, the electric field increases until the electrons gain a speed that is in excess of the speed of the ions. The dimensionless electron velocity is then greater than 1, which makes the electric field slope negative. The electric field therefore decreases (Hemmati 1995) until the electrons slow to speeds comparable to the ion speeds at the end of the sheath region ($\psi_2 \rightarrow 1$). This requires the electric field and its subsequent slope to approach zero at the sheath's end ($\eta_2 \rightarrow 0, \eta_2' \rightarrow 0$).

A trial and error method was utilized to integrate equations 16 through 19. For a given wave speed, α, a set of values for wave constant, κ, electron velocity, ψ_1, and electron number density, ν_1, at the shock front were chosen. The values of κ, ψ_1, and ν_1 were repeatedly changed in integrating equations 16 through 19 until the process lead to a conclusion in agreement with the expected conditions [9] at the end of the sheath region. A computer program was then used to calculate the ionization rate, μ, for the sheath region at each step of the integration. The conditions at the end of the sheath region were then used to find the equations that describe the quasi-neutral region, as had been done for proforce waves. To integrate the set of equations describing the quasi-neutral region, electron temperature, electron number density, and ionization rate values at the end of the sheath region were used as the initial boundary conditions for the quasi-neutral region. The computer program written for the sheath region was modified using the conditions given in [9], and as in the sheath region, ionization rate was calculated at every step of the integration of the EFD equations through the quasi-neutral region, making it possible to complete the necessary integration. Integration of the electron fluid-dynamical equations for antiforce waves was successful through both the sheath and quasi-neutral regions for wave speed values of $\alpha = 0.01$ and $\alpha = 2$, which represent wave velocities of 2.96×10^7 *m/s* and 2.10×10^6 *m/s*, respectively. For $\alpha = 0.01$, the initial boundary conditions required were $\kappa = 0.38$, $\psi_1 = 0.65$, and $\nu_1 = 0.04$. For $\alpha = 2$, the initial boundary conditions were $\kappa = 0.13$, $\psi_1 = 0.98$, and $\nu_1 = 0.45$.

Figure 1 depicts the electric field, η, as a function of position, ξ, within the sheath region with the electric field approaching zero as it nears the end of the sheath. For $\alpha = 0.01$ and $\alpha = 2$, the sheath region goes to $\xi = 1.95$ and $\xi = 8.44$, respectively, representing sheath thicknesses of 9.73×10^{-4} m and 2.12×10^{-5} m, respectively.

Figure 2 depicts electron velocity, ψ, as a function of position, ξ, within the sheath region. As expected, the dimensionless electron velocities for $\alpha = 0.01$ and $\alpha = 2$ go to one as they approach the end of the sheath region.

Figure 3 depicts ionization rate, μ, as a function of position, ξ, within the sheath region. For $\alpha = 0.01$ and $\alpha = 2$, the ionization rate goes to $\mu = 0.366$ and $\mu = 0.2$ at the end of the sheath region, respectively.

Figure 4 depicts electron temperature, θ, as a function of position, ξ, within the quasi-neutral region. The log of temperature and position is graphed for simplification. As expected, for both wave speeds at the end of the quasi-neutral region, the electron gas cools off to temperatures in which ionization is no longer possible ($\theta_f \rightarrow 0.065$). For $\alpha = 0.01$ and $\alpha = 2$, the final electron temperature goes to $\theta_f = 0.056$ and $\theta_f = 0.05$, respectively. $\theta_f = 0.056$ represent electron gas temperature of 3.24×10^4 K.

Figure 5 depicts electron number density, ν, as a function of position, ξ, within the quasi-neutral region. The log of position is graphed for simplification. As expected, the dimensionless electron number density approaches one ($\nu_f \rightarrow 1$) for both wave speeds at the end of the quasi-neutral region. $\nu_f = 1.0$ represents electron number density of 1.10×10^{20} / m^3.

Figure 6 depicts ionization rate, μ, as a function of position, ξ, within the quasi-neutral region. The log of position is graphed for simplification. For $\alpha = 0.01$ and $\alpha = 2$, the ionization rate goes to $\mu = 1.52 \times 10^{-6}$ and $\mu = 4.12 \times 10^{-7}$ at the end of the quasi-neutral region, respectively.

Conclusions

This research was successful in integrating the electron fluid-dynamical equations for antiforce waves through both the sheath and quasi-neutral regions. The results derived for wave speeds of $\alpha = 0.01$ and $\alpha = 2$ are consistent with the expected values at the end of both regions. Calculation of the ionization rate for the quasi-neutral region was successful by modifying the computer program written to calculate the rate at every step of

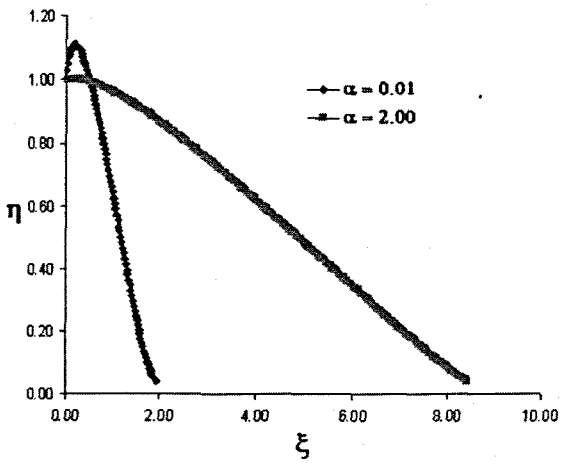

Fig. 1. Electric field, η, as a function of position, ξ, inside the sheath region for α = 0.01 and α = 2.

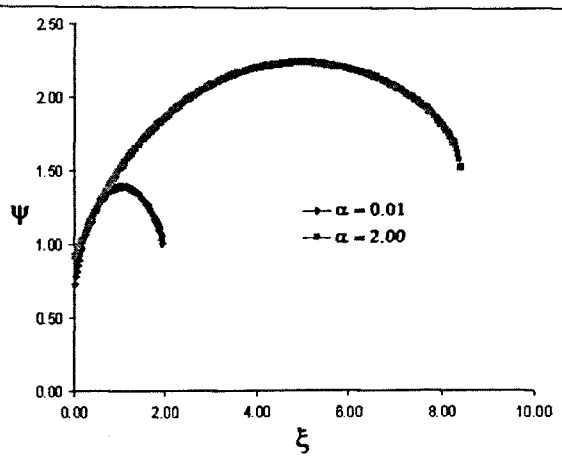

Fig. 2. Electron velocity, ψ, as a function of position, ξ, inside the sheath region for α = 0.01 and α = 2.

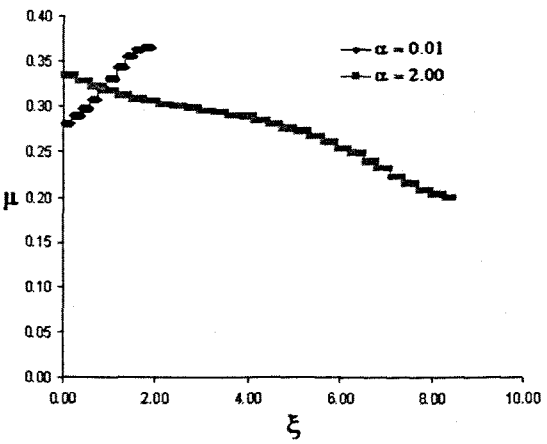

Fig. 3. Ionization rate, μ, as a function of position, ξ, inside the sheath region for α = 0.01 and α = 2.

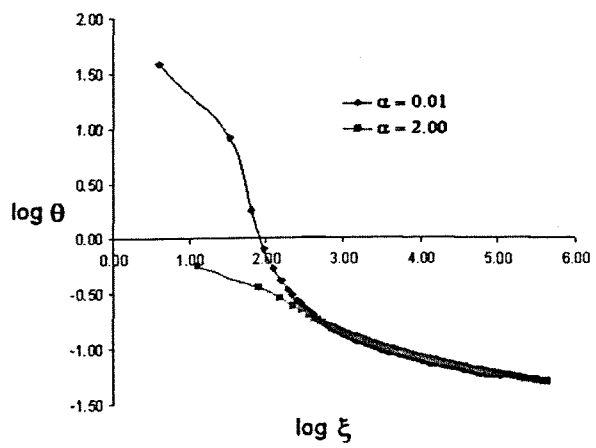

Fig. 4. Log of electron temperature, θ, as a function of log of position, ξ, inside the quasi-neutral region for α = 0.01 and α = 2.

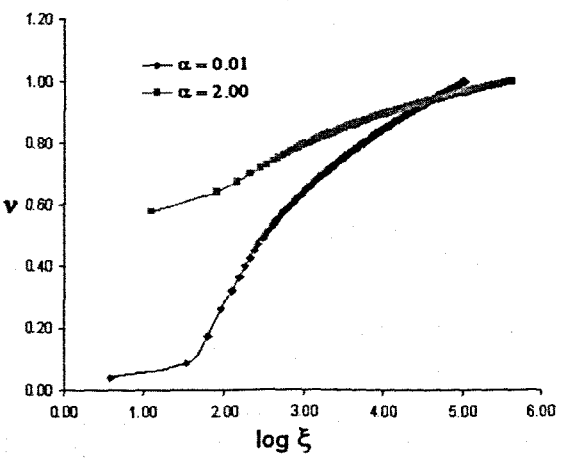

Fig. 5. Electron number density, ν, as a function of log of position, ξ, inside the quasi-neutral region for α = 0.01 and α = 2.

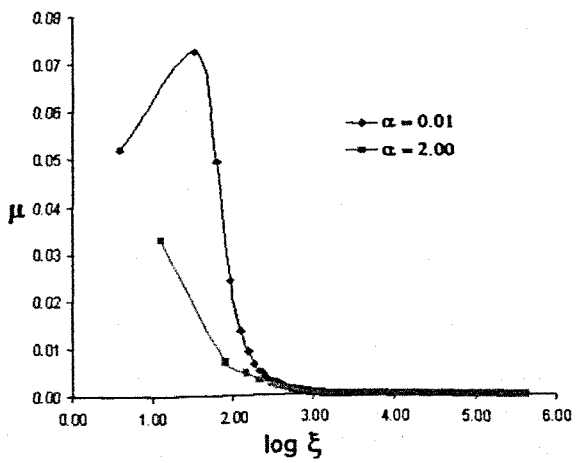

Fig. 6. Ionization rate, μ, as a function of log of position, ξ, inside the quasi-neutral region for α = 0.01 and α = 2.

the integration with the conditions known to exist at the end of the sheath. The wave speeds utilized and the calculated electron number densities, electron gas temperatures, and ionization rates all compare well with observations made by Uman et al. (1968), Rakov (2000), Fujita et al. (2003), and Brok et al. (2003), further confirming the validity of the fluid model used for breakdown waves.

ACKNOWLEDGMENTS.—The authors would like to express gratitude for the continued financial support offered by the Arkansas Space Grant Consortium for this area of research.

Literature Cited

Beams J W. 1930. The propagation of luminosity in discharge tubes. Physical Review 36:997-1002.

Blais RN and RG Fowler. 1973. Electron wave breakdown of helium. Physics of Fluids 16(12):2149-2154.

Brok WJM, J van Dijk, MD Bowden, JJAM van der Mullen, and GMW Kroesen. A model study of propagation of the first ionization wave during breakdown in a straight tube containing argon. Journal of Physics D: Applied Physics 36:1967-1979.

Fowler RG. 1983. A trajectory theory of ionization in strong electric fields. Journal of Physics B: Atomic and Molecular Physics 16:4495-4510.

Fowler RG and GA Shelton. 1974. Structure of electron fluid dynamical waves: proforce waves. Physics of Fluids 17(2):334-339.

Fowler RG, M Hemmati, RP Scott, and S Parsenajadh. 1984. Electric breakdown waves: Exact numerical solutions. Part I. The Physics of Fluids 27(6):1521-1526.

Fujita K, S Sato, and T Abe. 2003. Electron density measurements behind shock waves by H-β profile matching. Journal of Thermodynamics and Heat Transfer 17:210-216.

Haberstich A. 1964. Ph.D. Dissertation. Experimental and theoretical study of an ionizing potential wave in a discharge tube. University of Maryland, College Park, Maryland.

Hemmati M. and RG Fowler. 1985. Electric breakdown waves: exact solutions. Part II. The physics of Fluids. 28:2744-2750.

Hemmati M. 1995. Electron shock waves moving into an ionized medium. Laser and Particle Beams 13(3):377-382.

Hemmati M. 1999. Electron shock waves: speed range for antiforce waves. Proceedings of the 22nd International Symposium on Shock Waves; 1999 July 18-23; Imperial College, London, UK. Imperial College 2:995-1000.

Paxton GW and RG Fowler. 1962. Theory of breakdown wave propagation. Physical Review 128(3):993-997.

Rakov VA. 2000. Positive and bipolar lightning discharges: a review. Proceedings of the 25th International Conference on Lightning Protection 103-108.

Sanmann E and RG Fowler. 1975. Structure of electron fluid dynamical plane waves: antiforce waves. The Physics of Fluids 18(11):1433-1438.

Shelton GA and RG Fowler. 1968. Nature of electron fluid dynamical waves. The Physics of Fluids 11(4):740-746.

Thomson JJ. 1893. Recent Researchers. New York: Oxford University Press. p. 115.

Uman MA, RE Orville, and AM Sletten. 1968. Four-meter sparks in air. Journal of Applied Physics 39(11):5162-5168.

Von Zahn W. (Edited by G. Wiedemann.) 1879. Spectralrohren mit longitudinaler Durch-sicht. Annalen der. physic. 1-47:675-678.